Springer

Journal of Mechanical Science and Technology 22 (2008) 1490~1498

Journal of Mechanical Science and Technology

www.springerlink.com/content/1738-494x
DOI 10.1007/s12206-008-0413-x

Development of a wall-climbing robot using a tracked wheel mechanism

Hwang Kim, Dongmok Kim, Hojoon Yang, Kyouhee Lee, Kunchan Seo, Doyoung Chang and Jongwon Kim*

School of Mechanical and Aerospace Engineering, Seoul National University, Seoul, Korea

(Manuscript Received July 30, 2007; Revised March 27, 2008; Accepted April 16, 2008)

Abstract

In this paper, a new concept of a wall-climbing robot able to climb a vertical plane is presented. A continuous locomotive motion with a high climbing speed of 15m/min is realized by adopting a series chain on two tracked wheels on which 24 suction pads are installed. While each tracked wheel rotates, the suction pads which attach to the vertical plane are activated in sequence by specially designed mechanical valves. The engineering analysis and detailed mechanism design of the tracked wheel, including mechanical valves and the overall features, are described in this paper. It is a self-contained robot in which a vacuum pump and a power supply are integrated and is controlled remotely. The climbing performance, using the proposed mechanism, is evaluated on a vertical steel plate. Finally, the procedures are presented for an optimization experiment using Taguchi methodology to maximize vacuum pressure which is a critical factor for suction force.

Keywords: Climbing robot; Suction pad; Tracked wheel; Mechanical valve; Taguchi methodology

1. Introduction

The application of mobile robots in high places doing work such as cleaning outer walls of high-rise buildings, construction work, painting large vessels and inspecting storage tanks in nuclear power plants is required because they are currently performed predominantly by human operators and are extremely dangerous. For this reason, as a specific research field of mobile robotics, a number of climbing robots capable of climbing vertical surfaces have been researched and developed all over the world [1-4]. Most climbing robots developed at the present can be classified into two main functions: locomotion and adhesion. With an adhesive mechanism, climbing robots can attach to the wall by using suction force, magnetic force, micro-spines for interlocking and van der Waals force. The mechanism using magnetic force is only available when the climbing environment is composed of a ferromagnetic surface [4].

A robot using a micro-spine is able to attach to rough surfaces well, but cannot perform on a smooth surface like glass walls and ceilings [5]. A robot using van der Waals force mimics a Gecko's dry adhesion. This mechanism is novel and it requires no power for adhesion, but the value of the adhesion force is greatly affected by surface roughness, so it needs more research to insure its robustness actually [6]. Suction pads are widely used for industrial purposes and the most currently applicable and robust compared to other adhesive mechanisms.

In the case of locomotive mechanisms, they can generally be divided into legged mechanisms, sliding mechanisms and tracked wheel mechanisms. The advantage of the climbing robots employing a legged mechanism is that they can overcome uneven surfaces [2, 7]. But, they are comparatively heavy and the control system is complicated due to the number of actuators and gait control. These problems result in low speeds with discontinuous motion. Meanwhile, the realization of the sliding mechanism is relatively

*Corresponding author. Tel.: +82 2 880 7138, Fax.: +82 2 875 4848
E-mail address: jongkim@snu.ac.kr

simple in comparison with legged mechanisms, but its speed is also low due to discontinuous motion [3, 8]. Cleanbot II, developed by Zhu and Sun [1], which uses a tracked wheel mechanism, can move relatively fast with continuous motion. It employs a chain-track on which 52 suction pads are installed and each suction pad is controlled by a solenoid valve. But this robot has a large size, with a length of 720 mm, a width of 370 mm, and a height of 390 mm. It also has a heavy weight of 22kg, even if a power supply and a vacuum pump are not included in the robot. Furthermore, the maximum speed is 8m/min in spite of using the tracked wheel mechanism.

In this paper, a new concept of a climbing robot able to climb a vertical wall with continuous motion is presented. The locomotive motion with a high climbing speed is realized by adopting a series chain of two tracked wheels on which 24 suction pads are installed. Mechanical valves, installed on the robot instead of solenoid valves to control vacuum supply into suction pads, contributed to the improvement in climbing speed. It is a self-contained robot in which a vacuum pump and a power supply are integrated.

In this paper, the main mechanical structure based on engineering design [9], a wireless control and working principle of the tracked wheel mechanism are described, and then engineering analyses about the required suction force and the tendency of vacuum pressure in our system are presented. Experimental results such as climbing speed and payloads are described, and then the climbing performance using the proposed mechanism is verified. Finally, an optimization experiment to maximize vacuum pressure and minimize the fluctuation of vacuum pressure of the suction pads using Taguchi methodology is presented.

2. Design of robot system

2.1 Mechanical structure

As shown in Fig. 1, the robot is composed of a main frame and a tracked wheel system. On the main frame, a vacuum pump, power supply, control module and actuation set for driving are installed. The tracked wheel system is basically made up of a timing belt and pulley. Twelve suction pads and mechanical valves are installed on the outer surface of each timing belt and a guiding rail and profile cam, which guide the movement of suction pads according to wheel rotation and control the operation of mechanical valves, are fixed between wheel axes. Rotary joints located on either side of the robot prevent pneumatic tubes that link the vacuum pump to suction pads from twisting through wheel rotation. The rear axis of the wheel is connected to a geared BLDC motor and the power supply is installed at the bottom of the main frame. The main specifications of the robot are shown in Table 1.

Table 1. Specifications of the robot.

Items	Specification
Dimension	460 mm × 460 mm × 200 mm
Weight (including vacuum pump, power supply)	Approx. 14 kg
Max. climbing speed	15 m/min
Driving motor	1EA, Faulhaber BLDC, 200W (111:1)
Power supply	Li-ion polymer battery (25.9 V, 11 Ah)
Suction pad	24 EA, Ø60 mm
Vacuum pump	1 EA, N838_DC, KNF Max. flow rate: 32 L/min Max. vacuum pressure: 100 mbar abs.

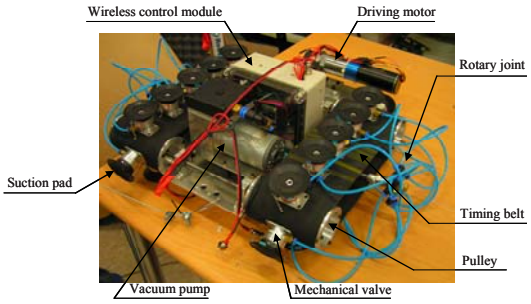

Fig. 1. Overall structure of climbing robot.

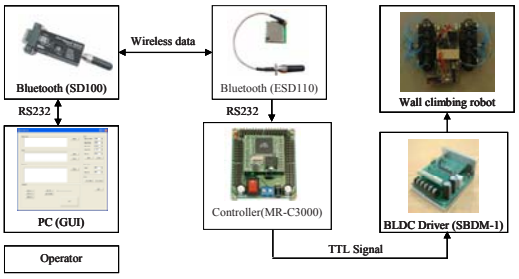

Fig. 2. Schematic of wireless control system.

2.2 Wireless control system

Since the on/off control of the valve is mechanically operated by wheel rotation, only the control of the driving motor such as start/ stop motion, change of direction and speed change is necessary. As shown in Fig. 2, connectors which follow Bluetooth v.1.2 protocol and the micro-controller which commands the BLDC motor driver are employed.

3. Working principle of tracked wheel mechanism

As mentioned above, the robot employs tracked wheels as the locomotive mechanism. It can move continuously as compared to climbing robots using a legged mechanism or sliding mechanism and that is why the climbing speed of this robot has been improved. The maximum climbing speed of our tracked wheel robot reaches 15 m/min.

As shown in Fig. 3, 12 suction pads and mechanical valves are installed on the outer surface of each timing belt and they are bolted with each follower. A guiding rail helps the follower move according to the wheel rotation without rocking from side to side. A curved profile cam located between the guiding rails controls the operation of mechanical valves. At the beginning, the mechanical valve is chocked because the spring inside of the valve closes up an opening. If a roller bearing located on the end of the valve is pushed down by the curved profile cam, free flow occurs between the vacuum pump and suction pad, and the suction pad attaches itself to the wall (Fig. 4).

The shape of the profile cam is designed to push the roller bearing when the suction pad approaches the wall and then the pad surface becomes parallel with the surface of the wall. Conversely, it releases the roller when the suction pad withdraws from the wall. This repetition of on/off operation of the valve enables the robot to climb the wall with fast and continuous motion.

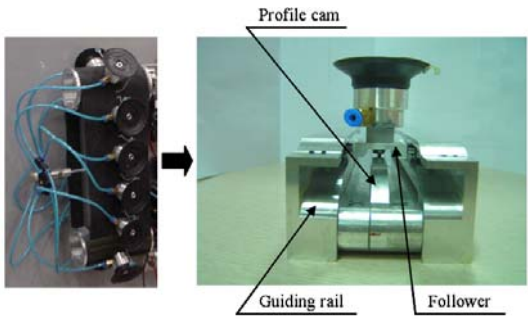

Fig. 3. Tracked wheel system.

4. Analysis

4.1 Analysis of the required suction force

To prevent the climbing robot from falling or slipping, sufficient suction force able to sustain the robot's weight is required. In this section, the conditions to prevent the robot's falling or slipping are addressed.

Fig. 5 shows the forces applied to the robot, when the robot attaches to a vertical steel plate.

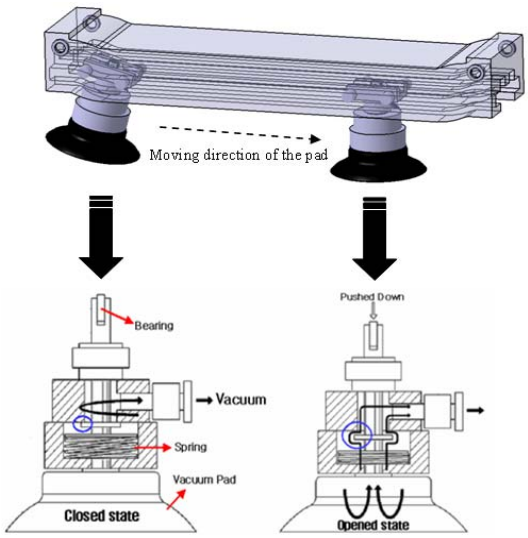

Fig. 4. Working principle of mechanical valve.

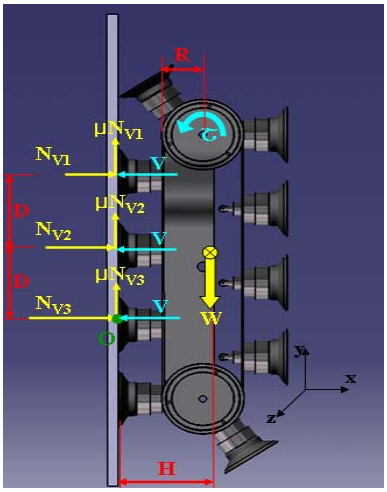

Fig. 5. Forces applied to the robot.

From a free body diagram of the robot as shown in Fig. 5, four equations for force and moment equilibrium are obtained. The force equilibrium in the x-direction is

$$\sum_{i=1}^{3} N_{vi} - 3V = 0 \tag{1}$$

Where V denotes vacuum force acting on each suction pad and N_{vi} represents normal reaction force acting on each suction pad. Likewise, the force equilibrium in the y-direction is

$$\mu \sum_{i=1}^{3} N_{vi} - W = 0 \tag{2}$$

where W means weight of the robot and μ denotes the friction coefficient. The moment equilibrium which bases point O in the z-direction is

$$HW + D(N_2 - V) + 2D(N_1 - V) = 0 \tag{3}$$

where D is the distance between two neighboring suction pads and H represents the distance from a wall to the center of gravity of the robot.

By assuming the robot is considered as a rigid body and the values of reaction forces acting on suction pads are in linear relation to each other, one more equation can be obtained. This is represented by

$$N_2 = \frac{N_1 + N_3}{2} \tag{4}$$

From these equations, the conditions to prevent the robot from falling or slipping can be obtained. Firstly, to prevent the robot from falling, the value of the reaction force should be positive.

$$N_i \geq 0 \tag{5}$$

Then, the smallest reaction force, N_1, can be obtained by solving (1)–(4) and (5) can be applied as follows:

$$N_1 = V - \frac{WH}{2D} \geq 0 \tag{6}$$

From (6), H is in proportion to N_1 and D is in inverse proportion to N_1. This means that the further the distance between two neighboring suction pads and the closer the distance from the wall to the center of gravity of the robot, the stronger the suction force obtained.

Secondly, to prevent the robot from slipping, the friction force should be greater than the gravitational force.

$$\mu \sum_{i=1}^{3} N_i - W \geq 0 \tag{7}$$

Substituting (1) into (7) yields the following result.

$$V \geq \frac{W}{3\mu} \tag{8}$$

Clearly, the robot will not fall or slip when the suction force satisfies the conditions of (6) and (8). When it comes to our robot, the total weight (W) is 14 kg, the distance between two neighboring suction pad (D) is 65mm, the distance from a wall to the center of gravity of the robot (H) is 80mm and the friction coefficient (μ) between the steel wall and suction pad is about 0.35. By substituting these values into (6), the required suction force not to fall is given as 84.38 N and the required suction force not to slip is given as 130.34 N. Therefore, the required suction force per pad not to slip or fall is 65.17 N. Since the real suction force used in the robot is about 137.2 N at the pressure of 400 mbar, it guarantees a safety factor of 2.12.

4.2 Tendency of vacuum pressure change

The vacuum pressure from the vacuum pump determines the suction force in the robot system. Therefore, a vacuum pressure able to maintain the required suction force is necessary in order to sustain the weight of the robot. In addition, there should not be any air leakage because the 24 suction pads used in the robot system are connected directly to the vacuum pump. In this robot system, the vacuum pump sucks the air that comes under volume inside the suction pad and the mechanical valve whenever different suction pads attach to the wall continuously by wheel rotation. From this periodic addition of the volume, fluctuation of pressure occurs which can exert a bad effect on the climbing performance of the robot.

To grasp the tendency of the pressure change, the simplified condition is modeled in Fig. 6.

For this basic model, the following equations are

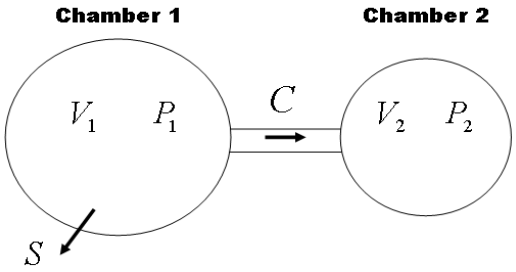

Fig. 6. Model of air flow.

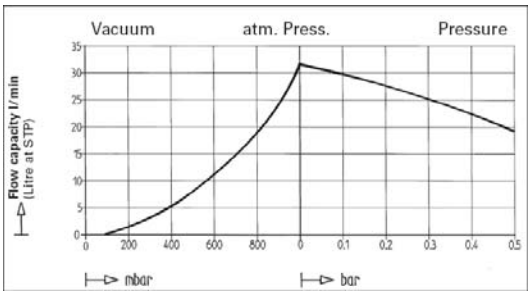

Fig. 7. Performance curve of the vacuum pump..

applied [10].

$$Q = PS = P(dV/dt) \tag{9}$$

where Q is gas throughput defined as the product of the pumping speed S, and the inlet pressure P, of the pipe. From Fig. 6, the throughput can be considered as

$$Q = C(P_1 - P_2) \tag{10}$$

where C is the conductance that depends on the kind of flow and the geometry of the pipe.

When there is only exhaust at chamber1, then the throughput balance equation based on (9) and (10) can be written as follows:

$$V_1 \frac{dP_1}{dt} = -SP_1 - C(P_1 - P_2) \tag{11}$$

$$V_2 \frac{dP_2}{dt} = C(P_1 - P_2) \tag{12}$$

When the robot climbs a vertical wall, Six suction pads are always attached to the wall and a different pair of suction pads repeats being attached and detached by turns. The former volume is selected as V_1 and the latter volume is selected as V_2. Fig. 7 shows

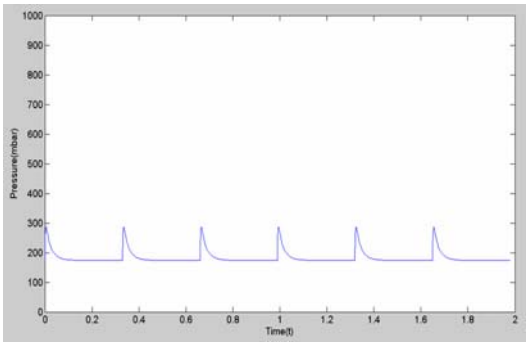

Fig. 8. Expected tendency of the pressure change.

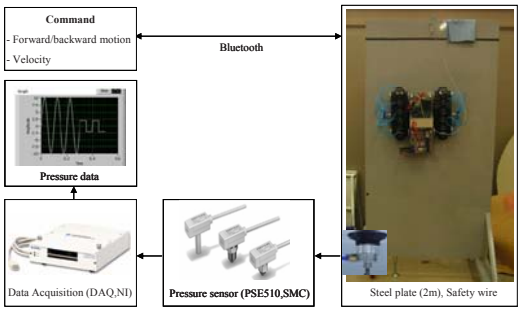

Fig. 9. Experimental setup.

a performance curve of the vacuum pump used in the robot. The volume flow rate (pumping speed) of the pump depends on the pressure. Fig. 8 shows the relationship between the pressure and time. The fact that pump pressure fluctuates with time when a regular volume is added periodically to the working vacuum pump is proven through this simplified simulation. This simulation is just to grasp the tendency of the pressure. The real value will be more critical because the shape of the pipe, the effect of the orifice and the minute leakage which determine the value of the conductance, are not considered.

5. Preliminary experiment

To confirm the climbing performance of the robot and to recognize the real pressure change, several experiments were conducted as shown in Fig. 9. The maximum climbing speed was measured at about 15m/min. While the robot is stopped, the loading capacity was about 200 N. The pressure applied to a single suction pad was measured as shown in Fig. 10.

The result shown is different than anticipated. The vacuum pump is not capable of sucking the air into the pump rapidly. This serious problem can lead to

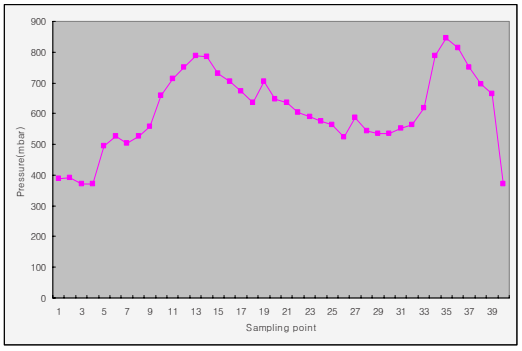

Fig. 10. Pressure change of a single suction pad (at a speed of 11.7 m/min).

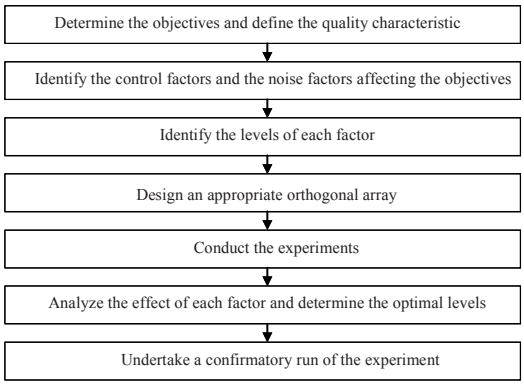

Fig. 11. The process of Taguchi methodology.

the robot falling or slipping because the required suction force to sustain the weight of the robot is not satisfied. An optimization experiment to improve this problem is discussed in the next part of this paper.

6. Optimization experiment

6.1 Taguchi methodology

To find an optimal design parameter by experiment, the most frequently used approach is a full factorial experiment. But this approach is time-consuming when there are many design factors. Taguchi methodology makes use of an experimental process for finding an optimal design. In this method, all factors affecting the performance quality can be classified into two types, such as control factor and noise factor. The former, being most important in determining the quality of product characteristics, can be determined by the experimenter and are easily controllable. The main issue is to find the control factors and determine their appropriate levels. For the robot system, typical control factors include the diameter of the pneumatic tube, the configuration of the profile cam, and the number of air tunnels inside the valve. The others, on the other hand, are undesired parameters that are difficult and impossible to control, such as climbing speed in the case of this experiment [11, 12]. Our experiment using Taguchi methodology follows the process as shown in Fig. 11.

6.2 Objectives and quality characteristics

From the preliminary experiment, the tendency of pressure change was not uniform and more critical than expectations. Maximizing vacuum pressure and minimizing the fluctuation of the pressure are determined as objectives to obtain the best climbing performance. As a quality characteristic, a smaller-the-better characteristic, in which the desired goal is to obtain a measure of zero, is applied to this experiment.

$$Y = \frac{1}{n}\sum_{i=1}^{n}\frac{1}{(P_i)^2} \tag{13}$$

where n means the number of experimental data and P_i is the vacuum pressure.

6.3 Control factors and noise factors

The objective of this experiment focuses on maximizing vacuum pressure and minimizing fluctuation of the pressure. Eventually, on/off timing of the valve and the air flow may have a significant impact on the pressure change. Therefore, three control factors are chosen: the diameter of the pneumatic tube, the configuration of the profile cam and the number of air tunnels inside the valve. In the case of the number of levels, three levels for each control factor are determined for fine tuning. The control factors and the levels are shown in Fig. 12 and Table 2. Meanwhile, the climbing speed is selected as a noise factor because the speed is not controllable and could have a desirable or undesirable effect on the vacuum pressure. The number of levels for the noise factor is fixed at two levels, which have a low speed and a high speed.

6.4 Orthogonal array

An orthogonal array is the basis for designing an experiment using Taguchi methodology. Unlike a full factorial experiment, an experiment based on an or-

Table 2. Control factors and noise factors.

Factor	Control factor			Noise factor
Item	Diameter of pneumatic tube (A)	Number of valve air tunnels (B)	Configuration of cam profile (C)	Climbing speed
Level1	8 mm	0 (5.13 mm^2)	47°	11.7 m/min
Level2	6 mm	1 (10.03 mm^2)	55.8°	5.2 m/min
Level3	4 mm	2 (14.98 mm^2)	40°	

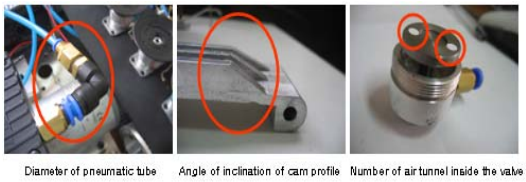

Fig. 12. Control factor features.

thogonal array is very efficient. $L_9(3^4)$, which is the most commonly used 3^n array, is selected because the number of control factors is three and there are three levels. Nine trials are carried out using the orthogonal array.

6.5 The experiments and analysis

From the experimental setup shown in Fig. 9, a pressure sensor is connected with a suction pad. The experiment is conducted by replacing each control factor and level shown in Table 2 based on the orthogonal array. Since the quality characteristic of this experiment is "the smaller the better," the equation for calculating the S/N ratio of this formulation is as follows.

$$S/N_{smaller-the-better} = -10\log(\frac{1}{k}\sum_{j=1}^{k} Y_{ij}^2) \quad (14)$$

where $k = 1,2$ means the level of noise factors, and $i = 1,2,\mathrm{L}\ 9$ presents the number of experiments based on the orthogonal array. Table 3 presents the results of the experiment. S/N ratios for each experiment can be obtained by (14). To produce the most desired results, it is necessary to identify control factors that have a strong effect on pressure. Since the effect of each control factor is the same as the difference between the average S/N ratio for each level, it can be presented by calculating the average experimental result for each level of control factor.

Table 3. Experimental data.

	Control factor			Output Y		S/N Ratio (dB)
	A	B	C	High speed	Low speed	
1	1	1	1	4.15	3.16	-11.33
2	1	2	2	5.03	3.61	-12.82
3	1	3	3	5.82	5.74	-15.24
4	2	1	2	3.64	2.71	-10.12
5	2	2	3	5.53	2.99	-12.96
6	2	3	1	5.77	4.72	-14.44
7	3	1	3	4.30	4.60	-12.97
8	3	2	1	7.41	5.89	-16.52
9	3	3	2	4.90	4.32	-13.29

Table 4. Response table (Significant factors in bold).

Level¥Control factor	A	B	C
1	-13.13	**-11.47**	-14.09
2	**-12.51**	-14.1	**-12.08**
3	-14.26	-14.32	-13.72
Difference	1.75	2.85	2.02

For example, -13.13 dB can be obtained by averaging the values of S/N ratios, which come under level 1 of control factor A. These results are shown in the response table (Table 4) and graph (Fig. 13) below.

The gap between extreme values informs how strongly the control factor impacts the quality characteristic. From Table 4, B has the strongest influence and A has the weakest influence on the value of S/N ratio. Thus, the combination of B1, C2, and A2 is recommended to get a high S/N ratio. Based on the selected levels having strong effects, an estimate of the predicted response can be computed. The calculations are based on the overall average experimental value defined as $\overline{T}$.

$$\overline{T} = \frac{1}{9}\sum_{i=1}^{9}(S/N)_i = -13.30 \quad (15)$$

Finally, prediction equation $\hat{\mu}$, defined as predicted S/N ratio based on the selected levels of the strong effects, can be written as (16).

$$\hat{\mu} = \overline{T} + (\overline{A2} - \overline{T}) + (\overline{B1} - \overline{T}) + (\overline{C2} - \overline{T}) = -9.46 \quad (16)$$

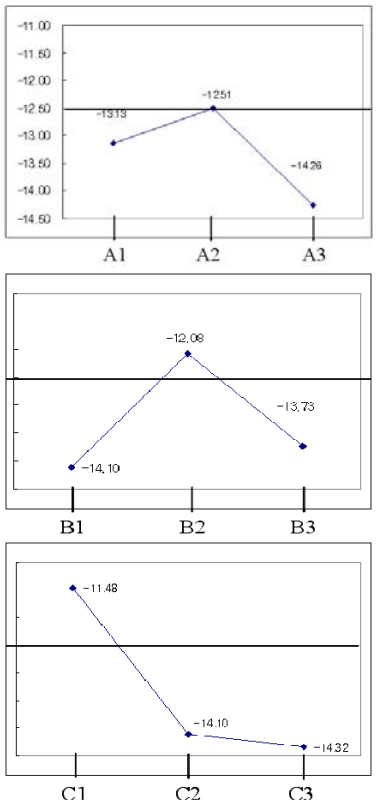

Fig. 13. Response graph.

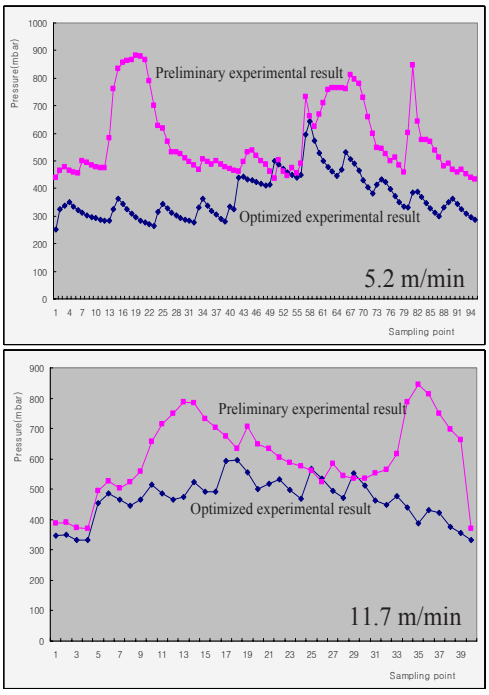

Fig. 14. Optimized results of vacuum pressure.

From these results, the recommended setting can be implemented because the actual results are close to the predicted results. Fig. 14 shows the improved result of the vacuum pressure using optimized factors. The total mean value of the vacuum pressure increased by 23.3% (143 mbar) and the gap between maximum pressure and minimum pressure decreased by 44% (208 mbar) at the speed of 11.7 m/min. When the speed is 5.3 m/min, the vacuum pressure increases by 35% (205 mbar) and the gap decreases by 12.7% (57 mbar).

7. Conclusion and future work

In this paper, a wall-climbing robot using a tracked wheel mechanism was presented. Continuous locomotive motion with high climbing speed is achieved by employing tracked wheels on which suction pads are installed. The engineering analysis and detailed mechanism design of the tracked wheel, including mechanical valves, was described. The climbing performance on a vertical steel plate using the proposed mechanism was evaluated. Finally, the procedures of an optimization experiment using Taguchi methodology to maximize vacuum pressure were introduced. From this experiment, performance related to suction force was improved and design parameters were optimized.

Now, a new research to develop a novel climbing robot able to adhere to rough surfaces and climb a 3-dimensional complex wall is in progress.

Acknowledgment

This work was supported by Brain Korea 21 program and Seoul R&BD program of Korea.

References

[1] J. Zhu nd D. Sun, S. Tso, 2002, Development of a tacked cimbing rbot, *Journal of Intelligent and Robotic Systems*, 35 (4) 427-443.

[2] S. Hirose, A. Nagakubo and R. Toyama, Machine that can walk and climb on floors, walls and ceilings, Proceedings of 5th International Conference on Advanced Robotics, 1 (1991) 753-758.

[3] H. Choi, J. Park, and T. Kang, A self-contained wall climbing robot with closed link mechanism, *Journal of Mechanical Science and Technology*, 18 (4) (2004) 573-581.

[4] Y. Wang, S. Liu, D. Xu, Y. Zhao, H. Shao and X. Gao, Development & application of wall-climbing robots, Proceedings of IEEE International Conference on Robotics and Automation, 1207-1212 (1999).

[5] S. Kim, A. Asbeck, M. Cutkosky and W. Provancher, Spinybot: climbing hard walls with compliant microspines, Proceedings of IEEE International Conference on Robotics and Automation, 601-606 (2005).

[6] S. Kim, M. Spenko, S. Trujillo, B. Heyneman, V. Mattoli and M. Cutkosky, Whole body adhesion: hierarchical, directional and distributed control of adhesive forces for a climbing robot, Proceedings of IEEE International Conference on Robotics and Automation, 1268-1273 (2007).

[7] B. Luk, D. Cooke, S. Galt, A. Collie and S. Chen, Intelligent legged climbing service robot for remote maintenance applications in hazardous environments, *Robotics and Autonomous Systems*, 53 (2) (2005) 142-152.

[8] N. Elkmann, D. Kunst, T. Krueger, M. Lucke, T. Böhme, T. Felsch and T. Stürze, SIRIUSc – Façade cleaning robot for a high-rise building in munich, germany, Proceedings of the 7th International Conference on Climbing and Walking Robots, 1033-1040 (2005).

[9] G. Pahl and W. Beitz, Engineering Design, Springer-Verlag (1997).

[10] A. Roth, Vacuum Technology, North-Holland, 3rd edition (1990).

[11] G. Peace, Taguchi methods: A Hands-on Approach to Quality Engineering, Addison-Wesley Publishing Company (1995).

[12] L. Zhao, H. Kim and J. Kim, Optimal design of smart panel using admittance analysis, *Journal of Mechanical Science and Technology*, 21 (4) (2007) 642-653.

[13] H. Zhang, J. Zhang, R. Liu, W. Wang and G. Zong, Design of a climbing robot for cleaning spherical surfaces, Proceedings of IEEE International Conference on Robotics and Biomimetics, 375-380 (2005).

[14] L. Kalra, J. Gu and M. Meng, A wall climbing robot for oil tank inspection, Proceedings of IEEE International Conference on Robotics and Biomimetics, 1523-1528 (2006).

[15] Z. Qian, Y. Zhao and Z. Fu, Development of wall-climbing robots with sliding suction cups, Proceedings of IEEE/RSJ International Conference on Intelligent Robots and Systems, 3417-3422 (2006).

[16] http://rodel.snu.ac.kr/wallclimbingrobot.asp